Precrystallization structures in supersaturated lysozyme solutions studied by dynamic light scattering and scanning force microscopy

Achim Schaper, Yannis Georgalis, Patrick Umbach, Jannis Raptis, and Wolfram Saenger

Citation: The Journal of Chemical Physics **106**, 8587 (1997); doi: 10.1063/1.473913
View online: http://dx.doi.org/10.1063/1.473913
View Table of Contents: http://scitation.aip.org/content/aip/journal/jcp/106/20?ver=pdfcov
Published by the AIP Publishing

Precrystallization structures in supersaturated lysozyme solutions studied by dynamic light scattering and scanning force microscopy

Achim Schaper[a)]
Max-Planck Institut für biophysikalische Chemie, Abt. Molekulare Biologie, Postfach 2841, 37018 Göttingen, Germany

Yannis Georgalis, Patrick Umbach, Jannis Raptis, and Wolfram Saenger
Institut für Kristallographie, Freie Universität Berlin, Takustr. 6, 14195 Berlin, Germany

(Received 4 December 1996; accepted 19 February 1997)

A comparitive study of the nanostructure evolving during aggregation of hen-egg white lysozyme in supersaturated solution was carried out by dynamic light scattering (DLS) and scanning force microscopy (SFM). Lysozyme aggregate (cluster) formation was observed in solution in the presence of NaCl, $(NH_4)_2SO_4$, and $NaNO_3$ as precipitating agents. The growth kinetics were examined by DLS and revealed fractal growth of the clusters with a fractal dimension of 1.8 obtained independently of the type of inert salt. Such behavior is typical for diffusion-limited cluster–cluster (DLCA) aggregation. Initial lysozyme cluster sizes were in the range of 12–35 nm. SFM images of individual lysozyme clusters at the liquid–solid interface were obtained in the presence of NaCl and $NaNO_3$ under crystallization conditions, and revealed cluster sizes in agreement with those determined by DLS. Extended domains of smaller sized clusters appeared on the mica surface after subjecting supersaturated lysozyme solutions to a dialysis step. The feasibility of DLS and SFM for monitoring the nano- and mesoscopic morphology of lysozyme aggregates in supersatured solutions and at the solid–liquid interface is discussed. © *1997 American Institute of Physics.* [S0021-9606(97)50620-9]

I. INTRODUCTION

Crystallographic protein structures at atomic resolution are indispensable for establishing structure–function relationships on the molecular level. However, the growth of protein crystals is a major obstacle in these endeavors. The temporal evolution of aggregation/precipitation under supersaturation yields bulk phase growth, which can be in general of polymorphic and/or isomorphic nature, leading to amorphous precipitation and/or crystallization, respectively. Crystallization proceeds via nucleation, propagation, and cessation.[1,2] During propagation, precipitation and crystallization are competing processes. The crystal formation depends critically on kinetic and thermodynamic constraints,[3] which are usually convoluted in a complex manner, making any prediction of suitable growth conditions extremely complicated.[4–6] An important observable in a crystallization essay is the appearance of microstructures, which typically occur in systems far from the thermodynamic equilibrium state.[7,8] The kinetic models employed for the interpretation of crystallization experiments do not account for such a transient structure formation. In contrast, thermodynamics describes growth phenomena close to equilibrium via compact structure formation via phase transition, thereby ignoring kinetic constraints. Therefore, for achieving more insight into the behavior of a molecular system under crystallization conditions, it is of primary importance to monitor the complete reaction path, from the first events of nucleation until the onset of bulk phase growth, using complementary methods that are sensitive to structure and dynamics.

Dynamic light scattering (DLS) provides direct means for determining the free-particle diffusion coefficient for ensembles of dilute, monodisperse particles in a stationary system (for review see Refs. 9–11). Time-resolved DLS measurements in a nonstationary system permit snapshots of the real time behavior of polymodal and polydisperse systems, provided the data acquisition time is shorter than the time scale of the chemical kinetics. Since this is usually not the case, only average size estimates are obtained for discrete time intervals of the data acquisition. The putative formation of microstructures during the initial states of crystal growth has been evidenced by light-scattering experiments and permits a fast inspection of crystallization assays.[12–15] It was recently shown that pertinent information can be obtained from DLS by introducing several tentative observables, including fractal dimension of the evolving microstructures.[16] The analysis of microstructure formation by DLS requires aggregate asymmetry corrections and extraction of the moments of size distribution.[14–17] Although it is difficult to discriminate between nucleation and propagation of crystal growth, there is strong evidence that postnucleation events can be monitored by DLS.

The direct observation of individual nuclei in a supersaturated solution requires imaging in liquid with nanometer spatial resolution. The scanning force microscope (SFM) is valuable tool for imaging the topography of biomolecules immobilized at the air–solid or liquid–solid interface (for a review see Refs. 18–20). SFM imaging yields a 3D repre-

[a)]Author to whom correspondence should be addressed. Tel: ++551 201 1765; Fax: ++551 201 1467; electronic mail: schaper@mpc186.mpibpc.gwdg.de

sentation of the surface. Due to its potential for imaging in liquid under native conditions, SFM has proven to be a promising method for the investigation of protein aggregates and individual proteins adsorbed to a solid surface.[21–23]

Lysozyme is a single chain molecule with a molecular mass of 14.3 kD. X-ray analysis reveals a compact ellipsoidal structure with dimensions $(4.5\times3\times3)$ nm^3 (see Ref. 24). The monomer self-diffusion coefficient in diluted aqueous solutions is 1.1×10^{-6} $(cm^2\ s^{-1})$ (see Ref. 25). Lysozyme is known to crystallize easily in the presence of NaCl and $NaNO_3$ but not in $(NH_4)_2SO_4$ (Refs. 26–28).

Macroscopic facet growth rates of lysozyme crystals have been reported, consistent with initial aggregate formation, mass transport to the crystal interface, and faceted crystal growth.[29,30] The growth of the facets of a microscopic lysozyme crystal in its mother liquor was also observed by SFM.[31–33] DLS studies revealed a transient formation of small oligomeric lysozyme aggregates during protein crystallization from a supersaturated solution.[12,13,16]

Lysozyme aggregates with radii between 21–25 nm were observed in saturated lysozyme solutions under crystallization conditions. Under optimum growth conditions the former were 12 to 15 times larger than the monomeric lysozyme.[16] From small-angle neutron scattering a mean lysozyme cluster radius up to 5 nm was revealed, dependent on the degree of supersaturation.[28] Thus, oligomeric lysozyme aggregates seem to be important intermediates during the process of crystal growth. In this study we combined DLS and SFM in order to examine the structure and morphology of lysozyme aggregates in the early states of crystallization and in the presence of different precipitation salts [NaCl, $NaNO_3$, and $(NH_4)_2SO_4$]. We show the complementary information can be obtained with respect to the appearance of precrystallization lysozyme clusters in supersaturated solutions by means of DLS, and by SFM imaging of the topography of a solid interface in continuous contact with a supersaturated lysozyme solution.

II. EXPERIMENT

A. Lysozyme preparation

The chemicals used in the present work of analytical grade. Deionized water was obtained from a Milli-Q water purification system (Millipore). Three times crystallization lysozyme was purchased from Sigma Chemical Co. (Deisenhofen, Germany). Aqueous solutions were dialyzed against water and lyophilized. All experiments were conducted in a 0.1-M Na-acetate, pH 4.2 buffer. NaCl, $(NH_4)_2SO_4$, and $NaNO_3$ p.a. grade, were purchased from Merck (Darmstadt, Germany). Monodispersity of the lysozyme solutions was verified by DLS at various protein concentrations under nonaggregating conditions.

B. Dynamic light scattering (DLS)

Protein and inert salt were rapidly mixed in appropriate ratios and filtered through Minisart sterile filters (220 nm pore size) into a standard cylindrical light scattering cell. DLS data collection started less than 1 min after mixing. DLS measurements were performed in an experimental setup equipped with a 2W Spectra Physics 2017 Ar^+ laser (operating at a wavelength of 488 nm) an ALV/SP-86 spectrogoniometer (ALV, Langen, Germany), and the ALV-FAST/5000/E digital autocorrelator boards. The scattering angle was 20° and the intensity autocorrelation function (intensity ACF) was accumulated for 30 s. All time-resolved experiments were performed at 20.0 ± 0.1 °C. The distribution of relaxation times was obtained by Laplace inversion of the normalized first order ACF with a modified version of the software package CONTIN,[34] as described elsewhere.[15] The mean radius of the growing aggregate was calculated from the mean relaxation time by applying the appropriately modified Stoke–Einstein relation for fractal clusters.[35]

C. Scanning force microscopy (SFM)

The samples were scanned with a NanoScope III multimode SFM [Digital Instruments (DI), Santa Barbara, CA] operated in the tapping mode using a J-scanner with a $135\times135(x,y)\times5(z)$ μm scan range. SFM measurements were done in liquid at room temperature (18–27 °C) using the fluid cell from DI. We used microfabricated Si-tips integrated into triangular cantilevers with a sensitivity (dF/dz) of ~0.1 N/m and a resonance frequency of ~160 kHz [Ultralevers, Park Scientific Instruments (Sunnyvale, CA)]. Images were obtained in the topographic (isoforce) mode. For imaging, the tip load was minimized by adjusting the damping amplitude to a minimum value. Images (512×512 pixels) were taken at a 5 Hz scan frequency. Image processing and data analyses were with the NanoScope software. A freshly cleaved mica surface (Muscovite type, Electron Microscopy Sci.) was used for support, and was premounted to the microscope. A lysozyme solution was mixed with the appropriate salt and 30 ml were immediately applied to the fluid cell (procedure 1). Small lysozyme aggregates and unconsumed monomers were removed by dialysis for 1 h against 50 mM Na-acetate pH 4.2, 0.75 M/NaCl, through a cellulose-ester membrane (Spectrapore, MW cutoff: 300 kDa; procedure 2). 50 ml of the dialyzed sample were injected into the fluid cell. The time period between mounting the sample to the fluid cell and scanning, i.e., the ''dead time,'' of the SFM experiment was typically between 5 and 10 min.

III. RESULTS

A. Diffusion limited cluster aggregation of lysozyme revealed by DLS

The first nucleation events of lysozyme aggregation under crystal growth conditions were examined. We have shown previously that the various observables, simultaneously plotted as a function of protein and salt concentration, exhibit pronounced extrema[17] that coincide with those solution conditions in which tetragonal (NaCl) and triclinic ($NaNO_3$) well-diffracting lysozyme crystals are obtained within less than 2 days.[5,26] Similar conclusions have been drawn from the triclinic ($NaNO_3$) lysozyme crystals, although the studies employing this type of inert salt have not

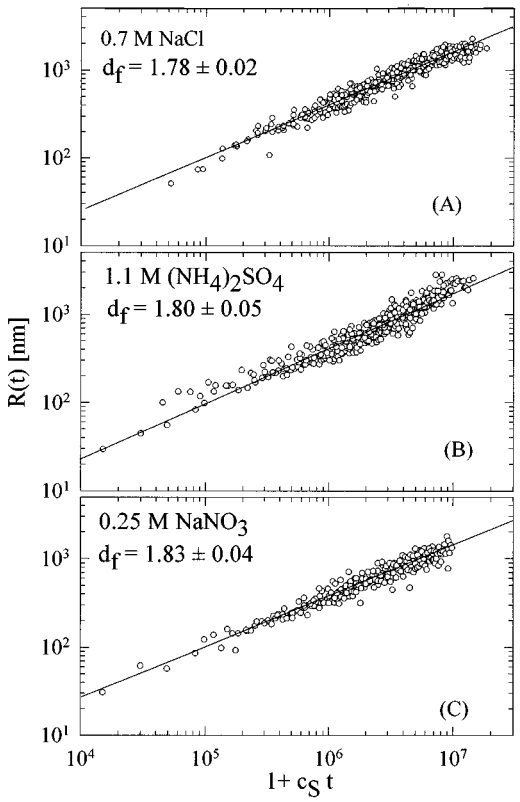

FIG. 1. Aggregation kinetics of lysozyme (0.34 and 2.74 mM) in the presence of 0.7 M NaCl (A), 1.1 M $(NH_4)_2SO_4$ (B), and 0.25 M $NaNO_3$ (C). (A) Eight time-resolved DLS data sets accumulated from 45 individual spectra were collected. The lysozyme concentration was varied between 0.34 and 2.74 mM with a step of 0.34 mM. (B) The lysozyme concentration was as in A. (C) Five time-resolved DLS data sets (45 spectra each) were collected. The lysozyme concentration was varied between 0.34 and 1.71 mM with an incremental change of 0.34 mM. The lines are least squares fits according to $\ln R(t)/\ln R(0) \sim (1/d_f)\ln c_s t$. The slope and intercept are equal to the reciprocal fractal dimension and initial aggregate size, respectively.

yet been conducted in such detail. DLS measurements were performed with aqueous supersaturated solutions of lysozyme and NaCl, $NaNO_3$, and $(NH_4)_2SO_4$ as precipitating agents [Figs. 1(A)–1(C)]. Aggregation proceeded undisturbed within 1 h with all electrolytes. Data analysis with CONTIN revealed a bimodal ACF. The relative amplitude of the fast mode decreased in time but the mean characteristic time constant was essentially constant. This hydrodynamic behavior was assigned to the monomeric (or even oligomeric) lysozyme as described in detail elsewhere.[15,36] In Figs. 1(A)–1(C) the time dependence of the mean cluster radius is displayed. The latter depends on the extent of aggregation and thus increases with time. Such behavior is expected for diffusion limited aggregation kinetics of lysozyme.[15,16] For a diffusion-limited cluster aggregation (DLCA) the scaling $R(t)$ is predicted by

$$R(t) = R(0)[1 + c_S t]^{z/d_f}, \tag{1a}$$

where $R(0)$ is the initial mean cluster radius, d_f denotes the fractal dimension of the aggregate, and c_S is the Smoluchowski rate constant given by

$$C_S = (4k_B T/3\eta)N_0\,, \tag{1b}$$

where $k_B T$ is the thermal energy, η is the solvent viscosity, and N_0 the initial number of molecules involved in the aggregation process. In Eq. (1a), z denotes a dynamic exponent that is associated with the reactivity between two clusters. Usually z is assumed to be 1 for a pure DLCA behavior. However, by small-angle SLS quite different values for z were observed, which could not be interpreted in terms of the classical aggregation theory.[37,38] According to Eq. 1(a), the determination of the fractal dimension requires linearization of the time behavior, which is readily achievable by a double logarithmic presentation. From Fig. 1, after linear regression of the data sets, the slope of the solid line can be identified with d_f ranging between 1.76 and 1.87, independent of the type of salt. From numerical calculations assuming small diffusing particles that collide with a nondiffusing aggregate (monomer–cluster aggregation), $d_f = 2.5$, and from a similar theoretical approach for cluster–cluster aggregation $d_f = 1.8$.[39,40] A fractal dimension of 1.8 was applied successfully in previous studies for modeling colloidal aggregation[41,42] and it is in excellent agreement with our data. From Fig. 1 the initial radius at different inert salt concentrations varied between 30 ± 5 nm for NaCl, 20 ± 5 nm for $(NH_4)_2SO_4$, and 15 ± 3 nm for the $NaNO_3$ clusters. The differences were small, albeit beyond experimental error, and presumably indicated structural differences and altered solvent mediated interactions between the different cluster types.

B. Imaging lysozyme aggregates under noncrystallization conditions by SFM

We investigated lysozyme adsorbates on mica during continuous contact with an under- or supersaturated lysozyme solution under crystallization conditions by SFM (procedure 1, see Materials and Methods). Control experiments with undersaturated solutions were performed in order to identify the morphological surface changes related to the lysozyme precipitation in an unambiguous manner. Figure 2(a) shows the mica surface exposed to the crystallization buffer without protein. The surface appeared corrugated homogeneously by colloidal salt precipitates with a corrugation amplitude <2 nm [cf. Fig. 2(d)], probably a consequence of the interfacial energy minimization between the negatively charged mica surface and the salt solution. In comparison, the bare mica surface was atomically flat and usually exhibited a corrugation amplitude in the subnanometer range (data not shown). After addition of an isotonic lysozyme solution to the sample Fig. 2(a), the morphology of the mica surface changed and oblate protrusions were exposed on a less corrugated surface [Fig. 2(b)]. The smaller particles were ~ 15 nm in lateral dimension and the larger extended to ~ 70 nm. Such particles, 3–5 nm in height [Fig. 2(e)], were never observed in the absence of protein. From this behavior, we inferred that the interfacial energy was modulated, due to the presence of protein, such that the amount of salt colloids adsorbed to the interface was reduced and partially replaced by protein. We conclude that this microscopic behavior is in agreement with the surfactant properties of proteins deduced

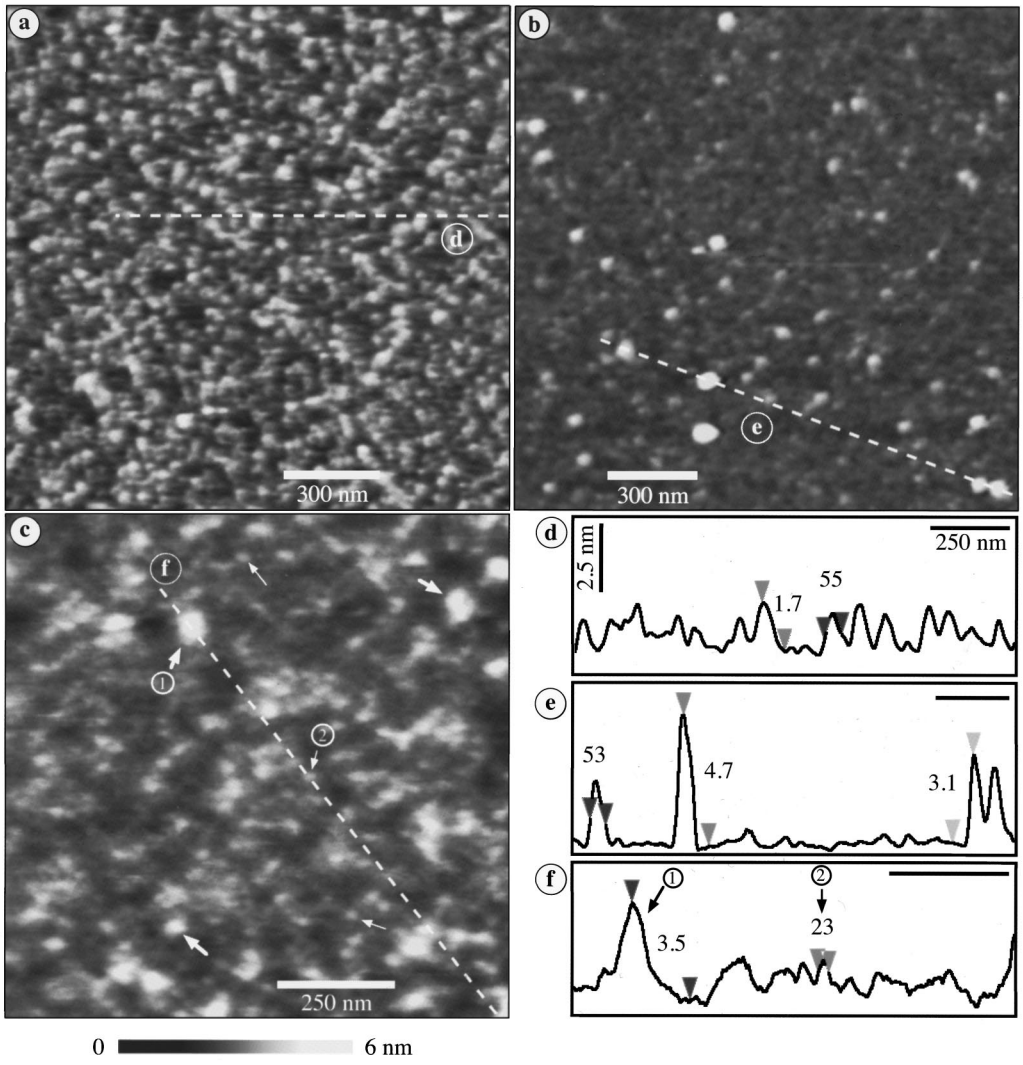

FIG. 2. SFM imaging in liquid of the individual components of the crystallization essay. Topview. The height is encoded according to the grey scale bar (in this case encodes for 6 nm). (a) The mica surface in contact with buffer 0.1 mM Na-acetate, pH 4.2, 0.15 M NaCl. (b) After addition of an isotonic lysozyme (35 μM, 0.5 mg/ml) solution to the sample in (a). (c) SFM image of the mica surface exposed to a pure lysozyme solution (2.1 mM, 3 mg/ml) in the absence of precipitating salt. Small arrows: oligomeric protein aggregate; large arrows: polymeric aggregate (d)–(f) Cross sections along the lines indicated in parts (a), (b), and (c). Horizontal scale bar =250 nm. Vertical scale bar =2.5 nm. Numbers are given for the vertical (horizontal) distance between markers.

from macroscopic observations. [In Fig. 2(c) a typical surface area is shown after incubation with lysozyme (3 mg/ml) in the absence of precipitating salt.] From the corrugated surface morphology, protein adsorption is indicated and a spectrum of sizes is visible. Typically, the adsorbates exhibited an oblate-like structure. The smallest particles [see Fig. 2(c), small arrows] extended only a few Å from the surface and had an apparent width of ~20 nm [cf. Fig. 2(f)]. The larger aggregates extended up to ~4 nm [see Fig. 2(f)] normal to the surface and varied in shape. From such aggregate dimensions we conclude that at least oligomeric lysozyme particles were apparent on the surface independent of the ionic strength. That is, lysozyme aggregation seems to be an intrinsic property of the system. It is possible that monomeric lysozyme also appears on the surface, but it is hard to differentiate between mono- and oligomeric states due to the limited resolution of the tip (tip-sample convolution, see Sec. IV). Figure 3 shows SFM images of the surface morphology at different protein and NaCl concentrations under suboptimal crystallization conditions. Typically, 5–10 min after injection of the protein solution, the surface structure was stable during repeated scanning, and images were acquired during the first hour of the precipitation process. Usually, the entire surface was covered with adsorbates. Figure 3(a) presents the surface relief at 3 mg/ml lysozyme concentration in 0.25 M NaCl. Individual lysozyme particles were visible with lateral dimensions between 50 and 70 nm [Fig. 3(e)]. Upon increasing the protein concentration to 30 mg/ml, Fig. 3(b), the surface density of those protrusions increased, and aggregates with more irregular shape appeared on the

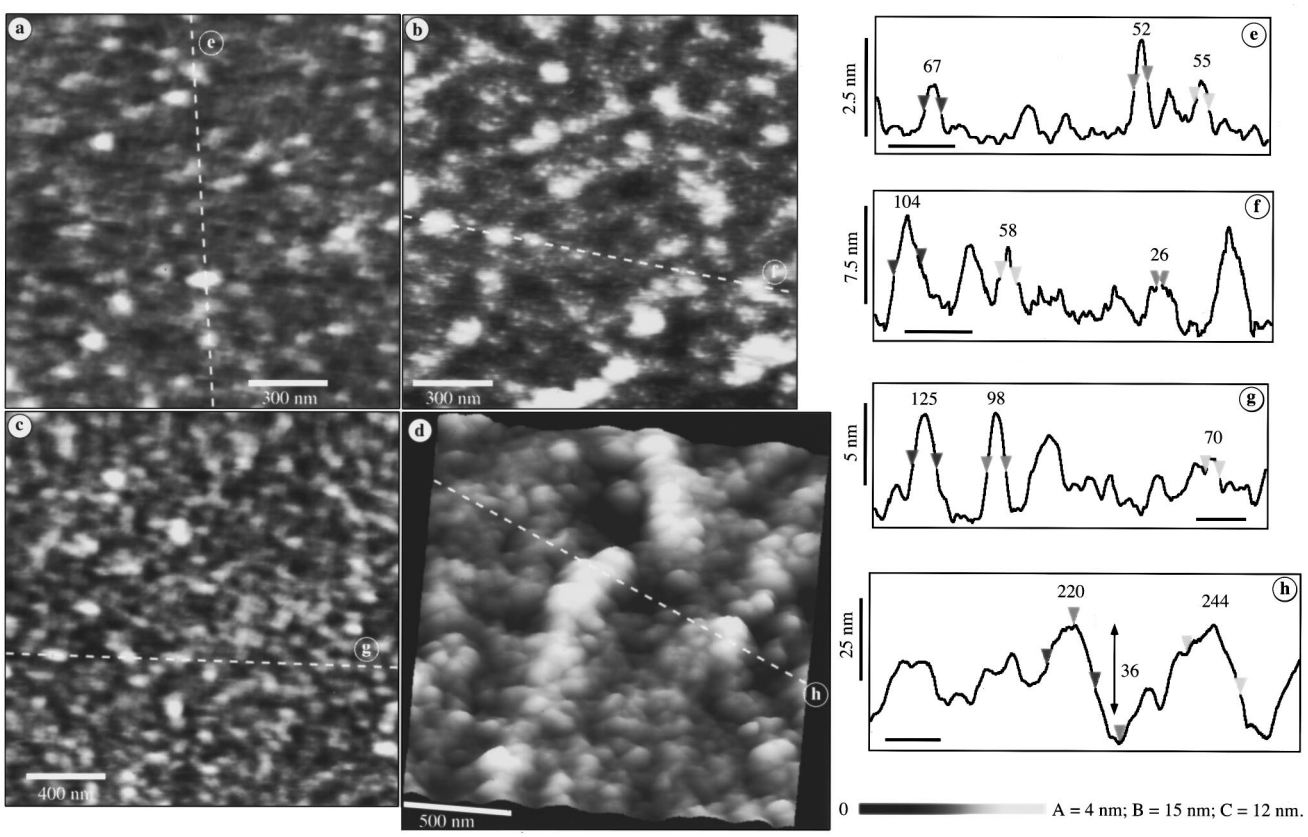

FIG. 3. SFM imaging in liquid of lysozyme precipitates under crystallization conditions. All solutions contained 0.1 M Na-acetate, pH 4.2. (a) 0.2 mM lysozyme (3 mg/ml), 0.25 M NaCl. (b) 2.1 mM lysozyme (30 mg/ml), 0.25 M NaCl. (c) 2.1 mM lysozyme, 0.5 M NaCl. (d) 5.6 mM lysozyme (80 mg/ml), 1 M NaCl. Under all experimental conditions a granular surface morphology was observed (for details see text).

surface varying between 50 and 100 nm in apparent diameter [Fig. 3(f)]. Interestingly, a subpattern of small round protrusions homogeneously distributed over the entire surface was obvious. The diameter of these particles was ~25 nm, and thus within the range expected for mono- and oligomeric lysozyme individuals [Fig. 3(f)]. As shown in Fig. 3(c), increasing the salt concentration of the lysozyme solution (30 mg/ml) to 0.5 M NaCl, led to the appearance of a granular topography. The surface consisted of protrusions with an apparent diameter in the range of 70–150 nm [Fig. 3(g)] homogeneously covering the mica surface. In Fig. 3(d) a compact and complex surface relief with tens of nm corrugation [Fig. 3(h)] was obtained after increasing both the lysozyme (80 mg/ml) and NaCl (1 M NaCl) concentration. A granular substructure was still obvious, which is typical for an aggregate growth by association of small particles.

Figure 4 shows a SFM image of lysozyme aggregates adsorbed to the mica surface in the presence of 0.4 M $NaNO_3$. From DLS measurements it is known that $NaNO_3$ is a strong precipitant and that multiple light scattering renders such experiments impossible at salt concentrations greater than 0.25 M (unpublished results). The aggregates observed in Fig. 4 were on average smaller compared to those in Fig. 3, with a mean apparent diameter between 30 and 40 nm (Fig. 4, cross section). In contrast to lysozyme aggregation induced by NaCl and $NaNO_3$, we were unable to detect adsorption of lysozyme clusters to the mica surface in the pres-

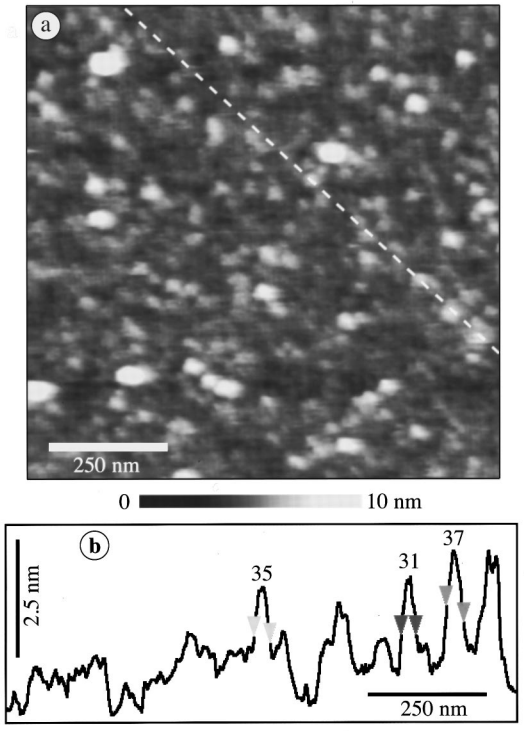

FIG. 4. SFM monitoring of lysozyme aggregates under crystallization conditions in the presence of $NaNO_3$. Conditions: 2.8 mM lysozyme, 0.4 M $NaNO_3$, procedure 1. The mean aggregate radius was ~20 nm. (a) topview, (b) cross section.

ence of $(NH_4)_2SO_4$, neither after direct injection into the fluid cell nor after dialysis (procedures 1 and 2). This result is compatible with the appearance of excess amorphous precipitates in crystallization assays of lysozyme and $(NH_4)_2SO_4$ (Ref. 43).

In Fig. 5(a) a selected area exhibiting a more regular surface pattern is shown. The latter extended ~500 nm in the lateral direction and ~2 nm (peak-to-peak) normal to the surface. In Fig. 5(b) the same region is shown after 3 min of continuous SFM imaging. Inspection of the differences between the topography in Figs. 5(a) and 5(b) revealed a few new features. In Fig. 5(c) the differential height contrast is presented, resolving more details about the growth process. As can be concluded from the dark contrast in small parts of the area, the height of a few regions remained essentially constant. Most of the differential area appeared in a brighter contrast (medium grey value corresponds to changes of ~5 nm), suggesting a continuous adsorption of protein at the surface during the scanning, which increased successively the thickness of the protein layer on the surface. In Fig. 5(d) a detail of the area indicated by the box in Fig. 5(b) is shown at higher magnification. The diameter of the protrusions was between 20 and 50 nm and thus comparable to the particle diameter expected for an oligomeric lysozyme aggregate. Thus our SFM data suggest that cluster growth proceeds by continuous deposition of smaller aggregates of comparable size, which are close to the initial cluster dimensions revealed by DLS.

IV. DISCUSSION

The combination of DLS and SFM allow for a first order analysis of the lysozyme aggregates and their growth under crystallization conditions. The results obtained from either technique were distinct but complementary. In a DLS experiment the aggregates are free to diffuse within the sample volume. The growth kinetics of the fractals were obtained by DLS with fair precision at the early stages of the reaction, i.e., within 1–2 hours, depending on the supersaturation level. Fractal growth can be described by power-law kinetics and the appearance of macroscopic crystals is reinforced within short times following a DLCA-like behavior. From DLS measurements it is not possible to discriminate between amorphous precipitation and crystallization, and thus the physical implications of fractal cluster growth with respect to crystal growth remain unresolved. In our previous work, and also in this paper, we interpreted $R(0)$ in Eq. (1a) in terms of an upper critical nucleus radius that does not exceed 30 nm for the lysozyme-NaCl system under optimal crystallization conditions. Up to now the morphology of such nuclei could not be predicted. However, from theoretical studies, deviations from the classical picture of the formation of a compact structure in the early states of a macroscopic crystal are expected.[39,44,45] In this context, restructuring is a very challenging possibility for obtaining microscopic crystals. For instance, STM studies of Ag aggregates[46] and low- and wide-angle x-ray scattering on zeolites,[47] indicated that nucleation transiently creates small fractal structures that undergo multiple restructuring toward a microscrystalline phase.

In contrast to our DLS measurements, SFM imaging was performed on lysozyme particles adsorbed to the mica surface. Mica has a negative surface charge density, which promotes *de novo* lysozyme adsorption under neutral and acidic pH (the isoelectric point of lysozyme is at pI 11) under noncrystallization conditions [cf. Fig. 2(c)]. In a control experiment, a positive charge density introduced by the spreading of the cationic detergent cethylpyridinium chloride[48] on the bare mica surface prior to the lysozyme incubation did not lead to protein adsorption. Such behavior of lysozyme is in agreement with SFM data from Radmacher *et al.*[23] and with results of studies in which a layer by layer assembly of multilayer films was realized by means of the alternate adsorption of lysozyme and anionic poly(styrene-sulfonate).[49] Based on this observation, we conclude that Coulomb interactions are involved in the adlayer formation of lysozyme particles. Such interactions are expected to have been unspecific under our experimental conditions (high salt leads to efficient charge screening) such that they did not interfere with the lysozyme (cluster) cohesion of subsequent adsorbed particles on top of the first layer on the mica surface. By SFM, the appearance of lysozyme aggregates was revealed clearly, with a mean lateral dimension similar to the mean diameter of initial clusters observed by DLS. From a mechanistic point of view we cannot differentiate between monomer and/or cluster adsorption events to the surface by means of SFM (see discussion below). Despite this limit in structural/temporal resolution, the simplest model for a theoretical description of the adsorption behavior of lysozyme monomers and/or clusters is diffusion limited adsorption generating self-affine structures. However, experiments involving rigorous image analysis are required in order to elucidate the morphology and the specific properties of the observed precrystallization clusters.

A. Limits in monitoring aggregation and crystallization by DLS and SFM

The aggregation of lysozyme proceeds on different time scales. The formation of initial lysozyme clusters is a fast process, probably occurring in the ms-range. Aggregation is much slower, i.e., requires hours, and is convoluted by crystallization, which takes place over several hours or up to days. Capturing the nucleation burst with time-resolved methods like DLS or neutrons scattering, may be extremely difficult due to the small size of monomeric lysozyme. The times required for completion of the primary nucleation burst are orders of magnitude shorter than the dead time of the DLS experiment. Gaining access to the short time limit requires the fast mixing, as e.g., stopped-flow techniques of classical kinetics, in combination with turbidity detection. In addition, the direct observation of critical nuclei for crystallization by DLS seems to be difficult due to the rare appearance of such structures compared to oligomers and fractal structures in such crowded solutions. Under special condi-

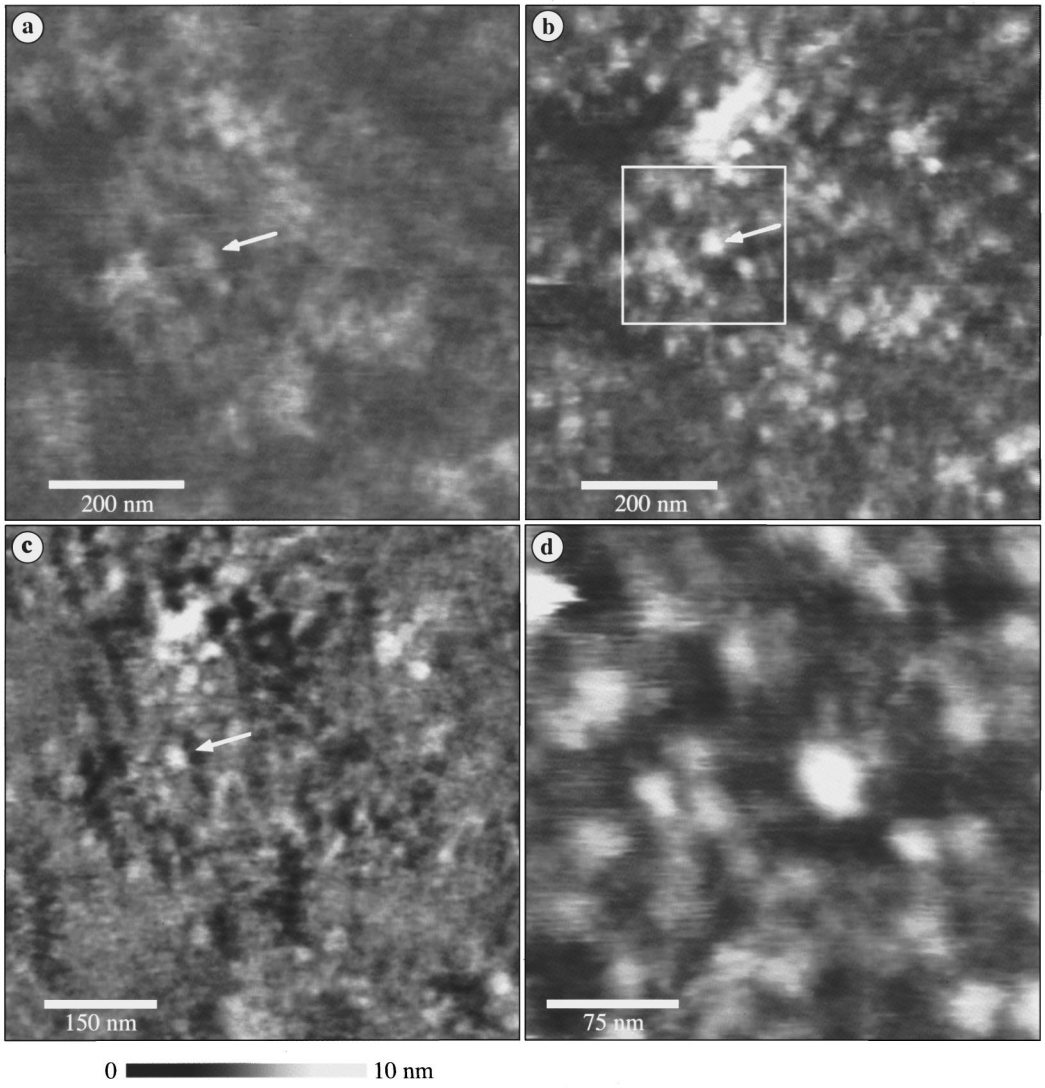

FIG. 5. SFM imaging of an individual lysozyme cluster at the liquid–solid (mica) interface after dialysis of a 5.6-mM lysozyme solution in 0.75 M NaCl (procedure 2). (a) Individual lysozyme cluster extending ~500 nm in lateral dimension. The cluster is built up from smaller particles with radii between 20 and 30 nm. (b) The same cluster as in (a) after 3 min of continuous SFM imaging. (c) Difference image (b)-(a) after proper alignment according to the fixpoint indicated by the arrow in (a) and (b). The differential height is grey scale encoded according to the horizontal scale bar. (d) Zoom of the surface area within the box indicated in (b) after 10 min of continuous scanning. The apparent particle diameter was about 20–40 nm.

tions, the observation of nuclei can also be accomplished by DLS when the fractals have reached a stationary size.

The dead time of the SFM experiment was 5–10 min after applying the solution to the fluid cell. This is mainly due to scanning instabilities, including thermal drift and convection, fragile surface structure, or transient tip contamination. Therefore, we did not have any access to the initial events of clustering. Another limitation is the finite time required for data acquisition, which was about 100 s per image in our case and thus compared with DLS. A specific difficulty assigned to SFM imaging is the maintenance of nondestructive imaging conditions during repeated scanning of the same surface area over hours. Since the tip is in continuous contact (interaction) with a surface region, this area is more or less obscured by the tip, which could perturb the aggregation process and thus the surface morphology. In addition, the tip load could be responsible for elastic depression of the surface relief, leading to a depletion of surface features. This could explain the appreciably reduced height of the adsorbed lysozyme from SFM metrology compared to its known dimensions from x-ray data. Last but not least, scanning instabilities leading to scan line distortions due to the amorphous character of the interface have to be taken into account. The lateral dimensions of imaged nanostructures are usually broadened by the tip due to geometric tip-sample convolution (the diameter of a fresh tip is typically in the range of 5 to 10 nm) and tip contamination by adsorbed particles. An interesting question is the appearance of crystal growth at the solid–liquid interface, i.e., epitaxial growth of facets under our experimental conditions. It is well known that proteins can be organized into two-dimensional arrays at a liquid–solid interface[50,51] and that 3D growth starts from such an adlayer.[52] We can only speculate about the appearance of two-dimensional lysozyme microcrystals at the mica surface

serving for nucleation centers for epitaxial growth, and of nonspecific nucleation induced by the high local protein concentration at the interface. Presumably the surface region in Fig. 5 reflects such an intermediate structure of the transition between bulk phase growth and amorphous precipitation.

V. CONCLUSIONS

We have shown that DLS and SFM are suitable techniques for the investigation of macromolecular aggregate formation. The average dimensions of the aggregates observed by SFM after induction of aggregation by NaCl or $NaNO_3$ were in fair agreement with the initial cluster sizes obtained by DLS. That is, the building unit of the fractals is not the lysozyme monomer but nanometer-size protein aggregates. Additional DLS and SFM experiments need to be performed in order to assess the size and shape of the evolving lysozyme clusters under crystallization conditions at various salt conditions. Such studies would lead to a better understanding of the rules governing the initial stages of protein crystallization. Finally, we would emphasize the central importance of the concept of fractal geometry as an important tool for the better understanding of the morphological transformations involved in the complex nature of crystal growth.

ACKNOWLEDGMENTS

We thank Dr. Thomas M. Jovin for critically reading the manuscript and Dr. Mario D. Soumpasis for stimulating this collaborative investigation. The financial support to A.S. and to Y.G. from the Deutsche Forschungsgemeinschaft (Jo 105/9 and Sa 196/26, respectively) is gratefully acknowledged.

[1] Z. Kam, H. B. Shore, and G. Feher, J. Mol. Biol. **123**, 539 (1978).
[2] G. Feher and Z. Kam, Methods Enzymol. **114**, 77 (1985).
[3] *Thermodyanmics and Kinetics*, edited by D. T. J. Hurle (North Holland, Amsterdam, 1994), Vol. 1.
[4] For cumulative references on protein crystallization diagnostics see Proc. J. Cryst. Growth **110** (1991); **122** (1992); Acta Cryst. **D50** (4) (1994).
[5] *Crystallization of Nuclei Acids and Proteints*, edited by A. F. Ducruix and R. Giegé (IRL, Oxford, 1992).
[6] R. Giegé, J. Drenth, A. F. Ducruix, A. McPherson, and W. Saenger, Progr. Cryst. Growth Char. **30**, 237 (1995).
[7] J. D. Gunton, M. San Miguel, and P. S. Sahni, in *Phase Transitions and Critical Phenomena*, edited by C. Domb and J. L. Lebowitz (Academic, New York, 1989), Vol. 8.
[8] D. W. Schaefer, B. C. Bunker, and J. P. Wilcoxon, in *Fractals in the Natural Sciences*, edited by M. Fleischmann, D. J. Tidlesley, and R. C. Ball (Royal Society of London, London 1989).
[9] S. K. Schmitz, *An Introduction to Dynamic Light Scattering by Macromolecules* (Academic, New York, 1990).
[10] B. Chu, *Dynamic Light Scattering* (Academic, New York, 1991), 2nd ed.
[11] *Dynamic Light Scattering, the Method and Some Applications*, edited by W. Brown (Oxford Science, Oxford, 1993).
[12] T. Azuma, K. Tsukamoto, and I. Sunagawa, J. Cryst. Growth, 371 (1989).
[13] M. Skouri, M. Delsanti, J. P. Munch, B. Lorber, and R. Giege, FEBS Lett. **295**, 84 (1991).
[14] Y. Georgalis and W. Saenger, Adv. Colloid Interface Sci. **46**, 165 (1993).
[15] Y. Georgalis, A. Zouni, W. Eberstein, and W. Saenger, J. Cryst. Growth **126**, 245 (1993).
[16] Y. Georgalis, J. Schüler, J. Franck, M. D. Soumpasis, and W. Saenger, Adv. Colloid. Interface Sci. **58**, 57 (1995).
[17] Y. Georgalis, J. Schüler, W. Eberstein, and W. Saenger, in *Fractals in the Natural and Applied Sciences*, edited by M. M. Novak (Elsevier Science B.V., Amsterdam, 1994), Vol. IFIP (A-41), p. 139.
[18] O. Marti and M. Amrein, *STM and SFM in Biology* (Academic, New York, 1993).
[19] R. Lal and S. A. John, Am. J. Physiol. **266**, C1 (1994).
[20] J. Yang and Z. F. Shao, Micron. **26**, 35 (1995).
[21] S. Karrasch, M. Dolder, F. Schabert, J. Ramsden, and A. Engel, Biophys. J. **65**, 2437 (1994).
[22] F. A. Schabert, J. H. Hoh, S. Karrasch, A. Hefti, and A. Engel, J. Vac. Sci. Technol. B **12**, 1504 (1994).
[23] M. Radmacher, M. Fritz, H. G. Hansma, and P. K. Hansma, Science **265**, 1577 (1994).
[24] D. C. Phillips, Proc. Nat. Acad. Sci. USA **57**, 484 (1967).
[25] S. B. Dubin, A. C. Noel, and G. B. Benedek, J. Chem. Phys. **54**, 5158 (1971).
[26] M. M. Riès-Kautt and A. F. Ducruix, J. Biol. Chem. **263**, 745 (1989).
[27] V. Mikol, E. Hirsch, and R. Giege, J. Mol. Biol. **213**, 187 (1990).
[28] N. Niimura, Y. Minezaki, M. Ataka, and T. Katsura, J. Cryst. Growth **154**, 136 (1995).
[29] A. Nadarajah, E. L. Forsythe, and M. L. Pusey, J. Cryst. Growth **151**, 163 (1995).
[30] M. R. Li, A. Nadarajah, and M. L. Pusey, J. Cryst. Growth **156**, 121 (1995).
[31] S. D. Durbin, W. E. Carlson, J. Cryst. Growth **122**, 71 (1992).
[32] S. D. Durbin, W. E. Carlson, and M. T. Saros, J. Phys. D **26**, B128 (1993).
[33] J. H. Konnert, P. Dantonion, and K. B. Ward, Acta Crystallogr. Sec. D **50**, 603 (1994).
[34] S. W. Provencher, Comput. Phys. Commun. **27**, 229 (1982).
[35] R. Klein, D. A. Weitz, M. Y. Lin, H. M. Lindsay, R. C. Ball, and P. Meakin, Progr. Colloid. Polym. Sci **81**, 161 (1990).
[36] W. Eberstein, Y. Georgalis, and W. Saenger, J. Cryst. Growth **143**, 71 (1994).
[37] D. Asnaghi, M. Carpineti, M. Giglio, and M. Sozzi, Phys. Rev. A, 1018 (1992).
[38] P. Umbach, Y. Georgalis, and W. Saenger, J. Am. Chem. Soc. **118**, 9314 (1996).
[39] W. Klein and F. Leyvraz, Phys. Rev. Lett. **57,** 2845 (1986).
[40] T. Vicsek, *Fractal Growth Phenomena* (World Scientific, New Jersey, 1989).
[41] D. A. Weitz and J. S. Huang, in *Kinetics of Aggregtaion and Gelation*, edited by F. Family and D. P. Landau (Elsevier, Amsterdam, 1984).
[42] M. Y. Lin, H. M. Lindsay, D. A. Weitz, R. C. Ball, R. Klein, and P. Meakin, Proc. R. Soc. London Ser. A **423**, 71 (1989).
[43] L. Vuillard, T. Rabilloud, R. Leberman, C. Berthet-Colominas, and S. Cusack, FEBS Lett. **353**, 294 (1994).
[44] D. W. Heermann and W. Klein, Phys. Rev. Lett. **50**, 1062 (1982).
[45] J. Yang, H. Gould, and R. D. Mountain, J. Chem. Phys. **93**, 711 (1990).
[46] H. Brune, C. Romainczyk, H. Röder, and K. Kern, Nature **369**, 469 (1994).
[47] W. H. Dokter, H. F. van Garderen, T. P. M. Beelen, R. A. van Santen, and W. Bras, Angew, Chem. **107**, 122 (1995).
[48] A. Schaper, J. P. P. Starink, and T. M. Jovin, FEBS Lett. **355**, 91 (1994).
[49] Y. Luvov, K. Ariga, and T. Kunitake, Chem. Lett. **12**, 2323 (1994).
[50] E. E. Uzgiris, Biochem. Biophys. Res. Commun. **134**, 819 (1986).
[51] E. E. Uzgiris, Biochem. Biophys. Res. Commun. **146**, 1116 (1987).
[52] S. A. Hemming, A. Bochkarev, S. A. Darst, R. D. Kornberg, P. Ala, D. S. C. Yang, and A. M. Edwards, J. Mol. Biol. **246**, 308 (1995).